

# Vibrational Spectra and Potential Functions of Cyclooctane and Some Related Oxocanes

Patrick W. Pakes,<sup>1a</sup> Thomas C. Rounds,<sup>1b</sup> and Herbert L. Strauss\*

Department of Chemistry, University of California, Berkeley, California 94720 (Received: February 27, 1981)

The infrared, far-infrared, and Raman spectra of cyclooctane and two oxygenated heterocycles are examined, giving special attention to the low-frequency region. Low-frequency ring-bending vibrations are calculated from the potential outlined in the preceding paper. The frequencies so calculated are consistent only with boat-chair structures for all three molecules. A complete normal coordinate analysis is performed on all three molecules using known force fields.

## Introduction

The conformations of saturated ring compounds are of continuing interest to chemists. As such, a wide variety of methods have been employed to determine their geometries and relative energies. Experiments such as nuclear magnetic resonance spectroscopy provide a check on the conclusions drawn from strain-energy minimizations but yield little information regarding the nature of the potential energy surface. To this end, vibrational spectroscopy has proved to be one of the few methods available for determining the detailed dependence of the energy on molecular geometry.<sup>2</sup>

Definitive analysis of the conformations of cyclooctane has been particularly challenging. Bellis and Slowinski in the previously available vibrational study<sup>3</sup> concluded that cyclooctane existed in the tub form by identifying fundamental bands and predicting the number expected for each symmetry, a method which is treacherous in practice. Although the molecule is now known not to be in the tub form, it can be inferred from this previous work that the molecule cannot be centrosymmetric. This conclusion is further supported by the observation of a small, but definite, dipole moment for cyclooctane in the gas phase.<sup>4</sup>

In the preceding paper,<sup>5</sup> a geometrical model of eight-membered rings together with a potential energy expression was described. The potential function was determined to provide relative energies and geometries of eight-membered rings consistent with other evidence and to reproduce the low-frequency vibrational spectra of the molecules presented in this paper. The potential function yields the boat-chair as the minimum-energy form for cyclooctane.

As in our previous work on smaller rings, we have used several mechanically similar molecules to provide more information on cyclooctane. These are the two cyclic ethers 1,3-dioxocane (C<sub>6</sub>H<sub>12</sub>O<sub>2</sub>) and 1,3,6-trioxocane (C<sub>5</sub>H<sub>10</sub>O<sub>3</sub>). Their optimized structures were also found to be boat-chairs with the oxygen atoms located in well-defined positions. The dioxocane has the 1,3 boat-chair structure and the trioxocane the 1,3,6, structure. These conformers are numbered by taking the bow of the boat as the 1 position and are discussed further in the preceding paper.<sup>5</sup>

The vibrational spectra are discussed in a number of steps. The anharmonic potential function for ring bending is first presented. The calculations for the low-frequency

vibrational frequencies for all three molecules are then discussed and compared with experimental values. In the development of the model to represent the potential energy of ring bending, an assumption was made that the motions of the ring atoms are relatively independent of other motions that occur in the entire molecule. To test this assumption and to further investigate the vibrational properties of rings, conventional normal coordinate analyses are carried out using known force fields. These calculations are then compared to the vibrational spectra.

## Calculations of the Conformations and the Low-Frequency Vibrations

We focus on the potential energy involved in ring deformations and on those vibrations that are most sensitive to conformational change. These vibrations involve the entire ring structure, and the relatively large masses coupled with weak restoring forces result in large-amplitude, low-frequency vibrations absorbing energy of less than 200 cm<sup>-1</sup> in the mid- and far-infrared region of the electromagnetic spectrum.<sup>6</sup>

The potential energy has been expressed in terms of the geometry of the ring in internal coordinates. The form of the potential used is

$$V(r, \theta, \tau) = \sum_{i=1}^8 \{ H_i(\psi_i - \psi_i^\circ)^2 + F_i(\psi_i - \psi_i^\circ) \times (\psi_{i+1} - \psi_{i+1}^\circ) + Q_i(\psi_i - \psi_i^\circ)^4 + T_i \cos 3\tau_i + K_i(\psi_i - \psi_i^\circ) \times (\psi_{i+1} - \psi_{i+1}^\circ) \cos \tau_i + \sum_{j=i+3 \text{ mod } 8}^{i+4} \sum_{m=1}^4 (Ae^{-r_{ijm}/r_0} - B/r_{ijm}^6) \} \quad (1)$$

where the  $\psi_i$  are the instantaneous values of the eight ring bond angles and the  $\psi_i^\circ$  are the values which they would have if the ring were opened. The  $\tau_i$  are the torsional angles. For cyclooctane, the  $r_{ijm}$  are the distances between nonbonded hydrogen atoms attached to carbon atoms  $i$  and  $j$  and the index  $m$  labels the four pairs of interactions. Additionally, this term accounts for oxygen-hydrogen interactions in the case of the cyclic ethers. The parameters used in this equation are presented in the preceding paper.<sup>5</sup>

This potential function is an effective one in the sense that it describes ring deformation only. The ring-bending vibrational frequencies were calculated in a harmonic approximation with the kinetic and potential energy matrix elements evaluated numerically by using the symmetry coordinates  $\omega_i$  of Figure 1.

## Experimental Section

**Preparations.** Cyclooctane was obtained as a reagent-grade solvent from Aldrich Chemical Co., Inc. (Milwaukee,

(1) (a) Materials Development Laboratory of General Motors, Corp., Flint, MI 48556. (b) Department of Biological Chemistry, Harvard Medical School, Boston, MA 02115.

(2) Rounds, T. C.; Strauss, H. L. *Vib. Spectra Struct.* 1978, 7, 238-68.

(3) Bellis, H. E.; Slowinski E. J., Jr. *Spectrochim. Acta* 1959, 12, 1103-17.

(4) Dowd, P.; Dyke, T.; Neumann, R. M.; Klemperer, W. *J. Am. Chem. Soc.* 1970, 92, 6325-7.

(5) Pakes, P. W.; Rounds, T. C.; Strauss, H. L. *J. Phys. Chem.*, preceding paper in this issue.

(6) Gwinn, W. D.; Gaylord, A. S. *MTP Int. Rev. Sci.: Phys. Chem., Ser. Two* 1976, 3, 205-62.

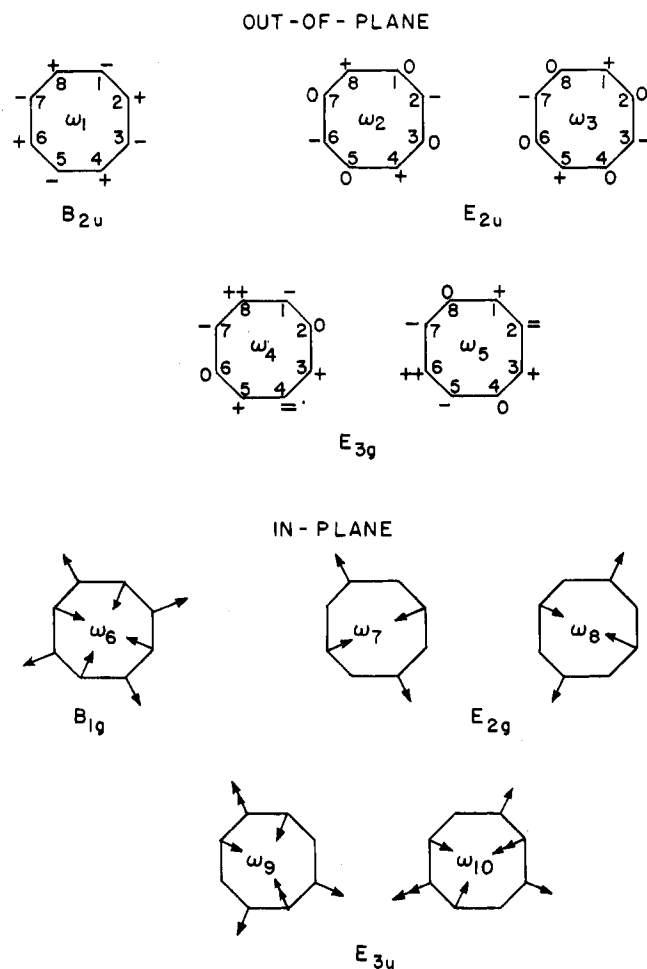


Figure 1. Vibrational symmetry coordinates for cyclooctane. The designations are for a planar  $D_{8h}$  molecule.

WI). Its composition was analyzed by gas chromatography, which revealed no significant impurities.

The heterocycles were synthesized according to the methods of Dale and Ekland<sup>7</sup> and Carothers and Hill.<sup>8</sup> In the preparation of 1,3-dioxocane, 1,5-pentanediol (2.0 mol), paraformaldehyde (1.2 mol), and 10 gm of 85% phosphoric acid were heated to 179 °C in a 250-mL flask with attached distilling apparatus for 2 h during which 30 mL of water was collected by distillation. The pressure was reduced to ~30 mmHg, and 30 gm of the product was collected at a boiling point of 60–70 °C. This product was again distilled through a Vigreux column at 45 °C and 10-mmHg pressure. The product was characterized by its NMR spectrum which gave a sharp singlet of relative intensity 1 at  $\delta$  4.6, an unresolved triplet of relative intensity 2 at  $\delta$  3.6, and a broad singlet of relative intensity 3 centered at  $\delta$  1.6 relative to tetramethylsilane ( $\text{Me}_4\text{Si}$ ).

In the preparation of the trioxocane, diethylene glycol (0.5 mol), benzene (150 mL), and 3 gm of Amberlite IR-120 cation-exchange resin in its acid form were heated in a 250-mL flask fitted with a water separator and a reflux condenser. The mixture was heated for 2 h and the resin was filtered off. The water formed was then collected off as the azeotrope, and the remaining benzene was evaporated under vacuum. The product distilled off at 60–70 °C at ~20 mmHg. It was further purified by fractional distillation. The yield was ~70%. Structure proof was

TABLE I: Observed and Calculated Ring-Bending Frequencies for Cyclooctane<sup>a</sup>

no.	calcd, $\text{cm}^{-1}$	obsd, $\text{cm}^{-1}$	
		infrared	Raman <sup>b</sup>
1	135 dp		125 dp
2	220 p	220	212 p
3	261 dp	255	245 dp
4	311 dp	295 <sup>c</sup>	292 dp
5	300 p	317 <sup>c</sup>	326 p
6	391 p	367 <sup>c</sup>	367 p
7	419 p	475	482 p
8	564 p	514	517 p
9	516 dp		540 dp
10	641 p		664 p

<sup>a</sup> All values in  $\text{cm}^{-1}$ . <sup>b</sup> p = polarized; dp = depolarized.

<sup>c</sup> These values taken from the liquid spectrum.

obtained from the NMR spectrum which had a singlet at  $\delta$  3.7 of relative intensity 4 and a singlet at  $\delta$  4.8 of relative intensity 1, with the chemical shifts relative to  $\text{Me}_4\text{Si}$ .

Both of these cyclic ethers were clear liquids with very camphoraceous odors. Gas chromatography revealed no detectable impurities in either distillate.

**Spectra.** The condensed-phase Raman spectra were obtained on the spectrometer of Dr. James R. Scherer. Data were obtained with signal averaging and at a resolution of 2  $\text{cm}^{-1}$ . Isotropic and anisotropic traces were obtained from the combination of polarized and depolarized spectra.

The infrared spectra were obtained on a variety of instruments. The condensed-phase far-infrared spectra were obtained on a Beckmann IR-11 spectrometer at a resolution of 4  $\text{cm}^{-1}$ . The vapor-phase spectra in the region 400–4000  $\text{cm}^{-1}$  were determined with a Nicolet 7199 Fourier transform spectrometer at 0.5- $\text{cm}^{-1}$  resolution. This instrument was fitted with a Wilks 20-m long-path cell.

The vapor-phase far-infrared spectra in the range 10–400  $\text{cm}^{-1}$  were obtained on a RIIC FS-520 Michelson interferometer which had been modified as described in the theses of Borgers,<sup>9</sup> Greenhouse,<sup>10</sup> and Pickett.<sup>11</sup> Mylar beamsplitters of 1/4- and 1/2-mil thickness were used to examine the regions 75–400 and 50–230  $\text{cm}^{-1}$ , respectively. Spectra were taken at a path length of 39 m in our multipass White-type cell<sup>12</sup> fitted with high-density polyethylene windows.

All of the vapor-phase infrared spectra were taken at room temperature at a sample pressure of ~4 torr except as noted below. The samples were first stored over molecular sieves to ensure dryness and then stored under vacuum after the air had been removed by several freeze-pump-thaw cycles.

**Spectral Assignments.** *Cyclooctane.* The far-infrared vapor-phase spectrum of the hydrocarbon revealed two very weak bands centered at 220 and 255  $\text{cm}^{-1}$ . The long-path cell was heated to ~70 °C in order to obtain enough absorption intensity for these to be seen. The low-frequency Raman spectrum of cyclooctane is shown in Figure 2.

The observed and calculated low-frequency ring-bending fundamentals for this molecule are outlined in Table I.

(9) Borgers, T. R. Ph.D. Dissertation, University of California, Berkeley, CA 1968.

(10) Greenhouse, J. A. Ph.D. Dissertation, University of California, Berkeley, CA, 1968.

(11) Pickett, H. M. Ph.D. Dissertation, University of California, Berkeley, CA, 1969.

(12) Pickett, H. M.; Bradley, G. M.; Strauss, H. L. *Appl. Opt.* **1970**, *9*, 2397.

(7) (a) Dale, J.; Ekland, T. *Acta Chem. Scand.* **1973**, *27*, 1519–25. (b) Dale, J.; Ekland, T.; Krane, J. *J. Am. Chem. Soc.* **1972**, *94*, 1389–90.

(8) Hill, J. W.; Carothers, W. H. *J. Am. Chem. Soc.* **1935**, *57*, 925–8.

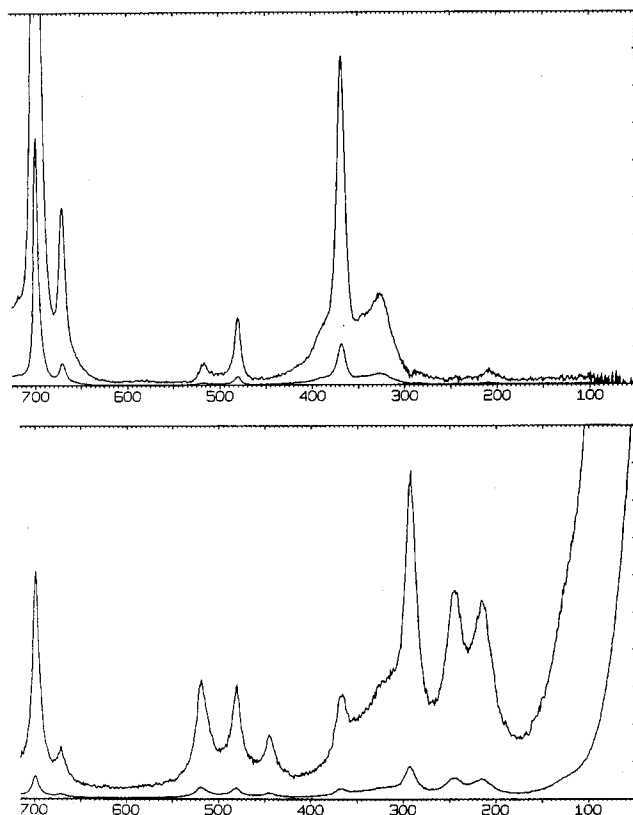


Figure 2. Low-frequency region of the Raman spectrum of liquid cyclooctane: (bottom) anisotropic spectrum; (top) isotropic spectrum.

The frequencies were calculated with the potential of eq 1 and with the geometry of the optimized boat-chair structure.<sup>5</sup> Vibrational calculations on other configurations of the cyclooctane molecule resulted in frequencies that did not fit the experimental observations. In particular, frequencies calculated for the crown forms were generally too low while those of the boat-boat were generally too high.

Boat-chair cyclooctane should have six symmetric and four asymmetric ring-bending vibrations, and six polarized and four depolarized bands were observed in the Raman spectrum that fit reasonably well with those calculated. For the  $C_8$  point group, all the vibrations are both infrared and Raman active and most of the transitions were found in both spectra.

A few of the normal coordinates of these ring-bending vibrations were rather complicated linear combinations of the symmetry coordinates of Figure 1. The normal coordinates for these 10 low-frequency motions of cyclooctane are shown in Figure 3.

**Cyclic Ethers.** The vibrational spectra of 1,3-dioxocane and 1,3,6-trioxocane have been reported<sup>13</sup> although there have been no detailed investigations. A portion of the far-infrared gas-phase spectrum of the dioxocane is shown in Figure 4, and the spectrum for the trioxocane appears in Figure 5. The excessive noise in Figure 4 is due to a noisy Golay detector. Low-frequency Raman spectra appear in Figures 6 and 7, for the dioxocane and the trioxocane, respectively.

The ring-bending frequencies for these molecules were calculated as for cyclooctane. The fundamentals in the spectrum were assigned and are shown in Tables II and III along with calculated results for the minimum-energy

#### LOW-FREQUENCY NORMAL COORDINATES

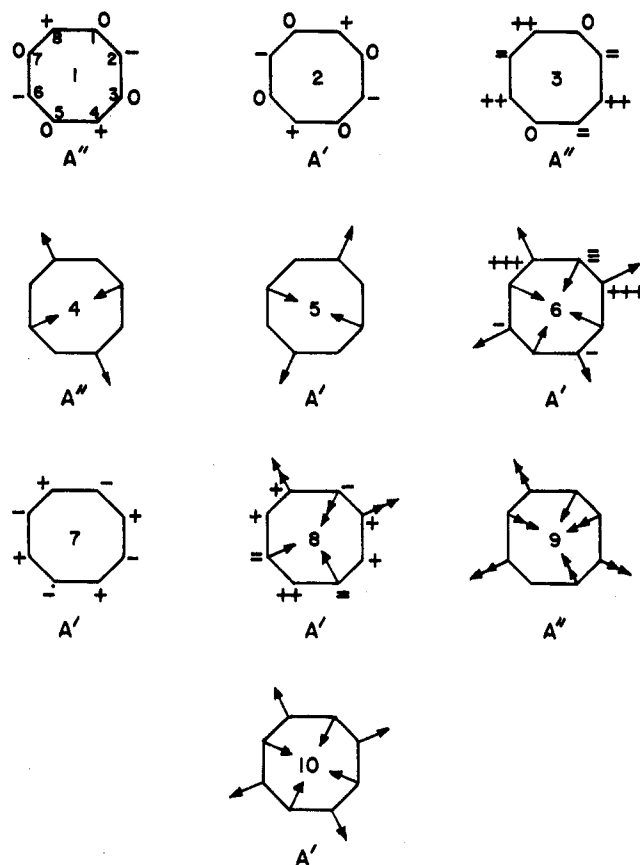


Figure 3. Sketch of the calculated normal coordinates of cyclooctane. Position 1 is the bow of the boat-chair. Since the molecule is not planar, the "in-plane" and "out-of-plane" motions mix; the symmetry designations are for the plane of symmetry of the boat-chair. The approximate correlations of the diagrams to the coordinates of Figure 1 are as follows: drawing 1 corresponds to  $\omega_1$ , 2 to  $\omega_3$ , 3 to  $\omega_4$ , 4 to  $\omega_7$ , 5 to  $\omega_8$ , 6 to a mixture of  $\omega_5$  and  $\omega_9$ , 7 to  $\omega_1$ , 8 to a mixture of  $\omega_5$  and  $\omega_9$ , 9 to  $\omega_{10}$ , and 10 to  $\omega_6$ .

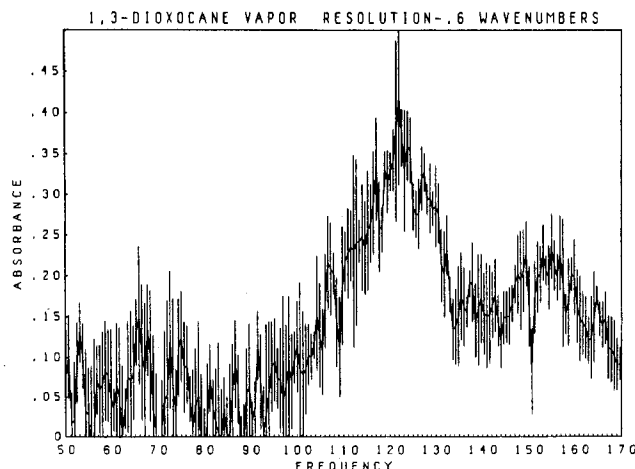


Figure 4. Far-infrared spectrum of 1,3-dioxocane. An average of three sample traces and background traces. Error bars denote one standard deviation.

boat-chair 1,3 and boat-chair 1,3,6 forms. These conformers are asymmetric, and all of the Raman bands should be partly polarized. However, many bands observed were nearly totally depolarized, and we characterize these bands as "depolarized" in the tables. A reasonable hypothesis is that these molecules maintain a pseudoplane

(13) Tarte, P.; Laurent, P. A.; Rogister-Paris *Bull. Soc. Chim. Fr.* 1960, 365-9.

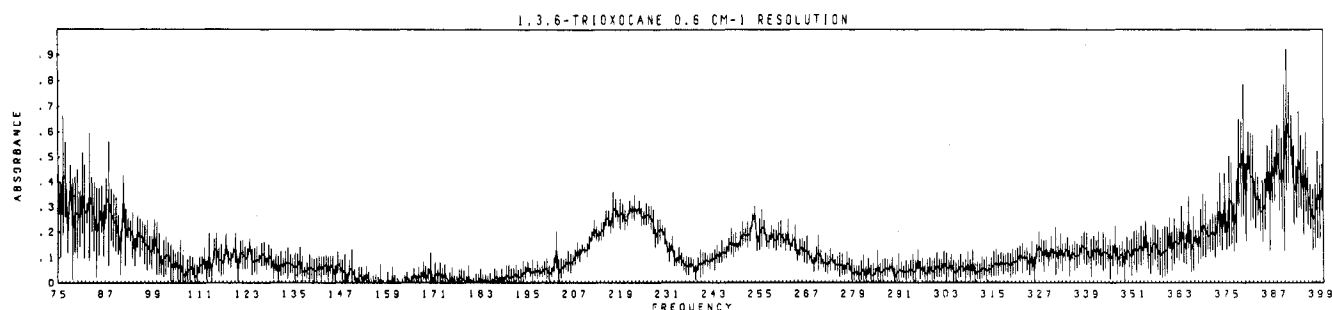


Figure 5. Far-infrared spectrum of 1,3,6-trioxocane. An average of three sample traces and three background traces.

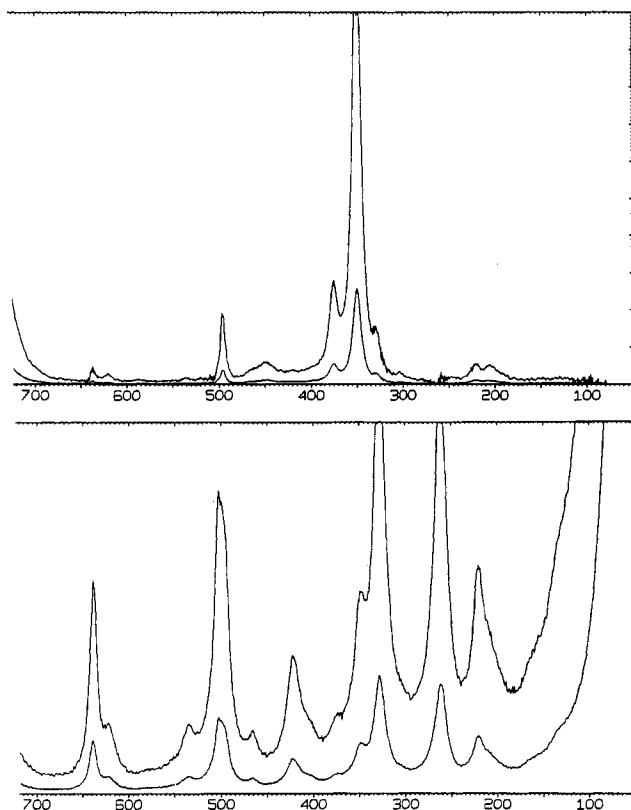


Figure 6. Low-frequency Raman spectrum of 1,3-dioxocane: (bottom) anisotropic part; (top) isotropic part.

TABLE II: Observed and Calculated Ring-Bending Frequencies for 1,3-Dioxocane<sup>a</sup>

calcd	obsd	
	infrared	Raman
143	120	135 dp
222	220	225 dp
255	254 <sup>b</sup>	267 dp
276		305 p
338	344 <sup>b</sup>	347 p
383	374 <sup>b</sup>	372 p
431	419	422 dp
533	501	497 p
593	533	535 dp
665	639	637 dp

<sup>a</sup> All values in  $\text{cm}^{-1}$  (the designations p and dp are approximate; see text). <sup>b</sup> Taken from condensed-phase spectrum. All other values from vapor-phase spectrum.

of symmetry during execution of their low-frequency normal vibrations and that an oxygen atom is dynamically equivalent to a methylene group. Inspection of the calculated eigenvectors revealed no apparent plane of symmetry, and no correlations with the observed polarizations

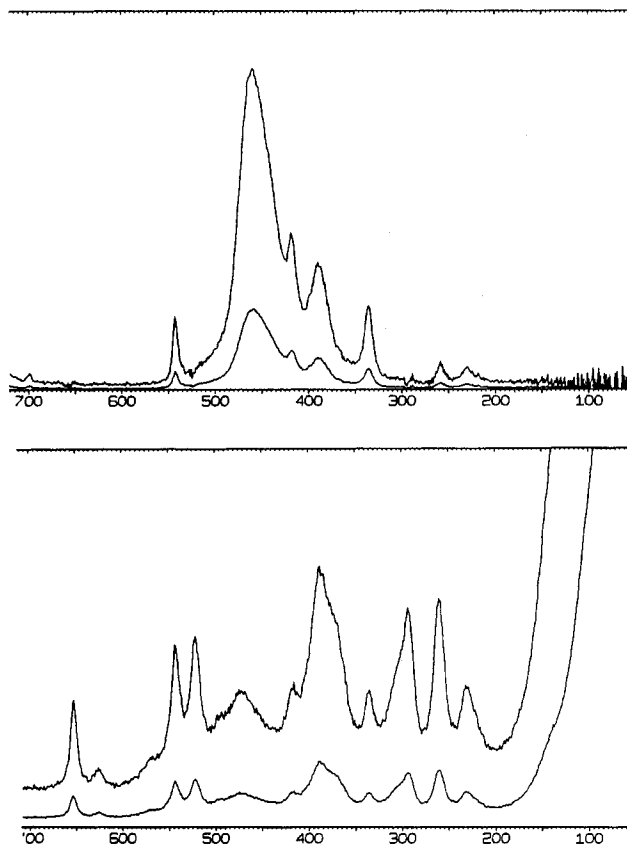


Figure 7. Low-frequency Raman spectrum of 1,3,6-trioxocane: (bottom) anisotropic part; (top) isotropic part.

TABLE III: Observed and Calculated Ring-Bending Frequencies for 1,3,6-Trioxocane<sup>a</sup>

calcd	obsd	
	infrared	Raman
137	122	137 dp
230	223	230 p
266	256	260 p
280		295 dp
352	337	335 p
395	390	385 p
445	440	460 p
536	537	518 dp
565		542 p
665	655	651 dp

<sup>a</sup> All values in  $\text{cm}^{-1}$  (the designations p and dp are approximate; see text).

could be made. The normal coordinates for the low-frequency vibrations of these molecules are very similar to those of cyclooctane, but in general asymmetric.

*Nonfundamental Low-Frequency Vibrations.* Both the six-membered<sup>14</sup> and seven-membered<sup>15</sup> rings show sum and

TABLE IV: Low-Frequency Nonfundamental Bands

obsd frequency, $\text{cm}^{-1}$		
infrared	Raman	assignment
Cyclooctane		
440 vw	442 dp, w	$2 \times 220 = 440?$
1,3-Dioxocane		
155 w	155 dp, vvw	$422 - 267 = 155$
	207 p, vw	$347 - 135 = 212$
	328 dp, w	
442 vw		$2 \times 220 = 440$
468 w	465 dp, vw	$220 + 254 = 474$
1,3,6-Trioxocane		
70 w		difference band (?)
375 m	372 p, m	$137 + 230 = 367$
	418 p, vw	$137 + 295 = 432 (?)$
	472 dp, vw	$137 + 335 = 472$
	495 p, vw	$230 + 260 = 490$
	625 dp, vw	?

difference bands involving the low-frequency out-of-plane modes together with miscellaneous other ring modes. Similar bands are found for the eight-membered rings and are listed in Table IV together with possible assignments. For cyclooctane itself, the symmetry provides a guide, and for the oxocanes the pseudosymmetry was used. The band at  $\sim 440 \text{ cm}^{-1}$  in dioxocane fits nicely as an overtone of the  $220 \text{ cm}^{-1}$  fundamental. We make this tentative assignment of the cyclooctane band as well, even though it appeared to be depolarized. The trioxocane shows a weak band at  $70 \text{ cm}^{-1}$ , the region of the spectrum in which bands due to free or slightly hindered pseudorotation are to be expected. The NMR evidence suggests the presence of a crown family conformer in the trioxocane, and this conformer may pseudorotate rather freely.<sup>5</sup> The  $70\text{-cm}^{-1}$  band could be a pseudorotation band of the crownlike conformer. However, there is no other feature indicative of free pseudorotation of the trioxocane. Furthermore, the infrared spectrum of the trioxocane is comparatively strong because of the presence of the ring oxygens, and so the  $70\text{-cm}^{-1}$  band might be just an unspecified difference band of the boat-chair.

### Complete Normal Coordinate Analysis

For cyclooctane, the valence force field derived from the vibrational analysis of saturated hydrocarbons by Snyder and Schachtschneider<sup>16</sup> This force field was deemed appropriate in that the frequencies of cyclohexane and adamantane were included in its fit, and its application to the twist-chair of cycloheptane gave excellent correlation to the observed frequencies.<sup>15</sup>

The geometry used in the calculation was that of the optimized boat-chair.<sup>5</sup> All bend-bend interaction force constants of  $<0.02 \text{ mdyne}/\text{\AA}^2$  were ignored. The frequencies were computed with eq 1 using programs GMAT and FPRT.<sup>17</sup> As a check on the accuracy of computation, a second normal coordinate program, NORCRD,<sup>18</sup> was used.

(14) Pickett, H. M.; Strauss, H. L. *J. Chem. Phys.* **1970**, *53*, 376-88.

(15) Bocian, D. F.; Strauss, H. L. *J. Am. Chem. Soc.* **1977**, *99*, 2866-76.

(16) Snyder, R. G.; Schachtschneider, J. H. *Spectrochim. Acta* **1965**, *21*, 169-95.

(17) Schachtschneider, J. H. "Vibrational Analysis of Polyatomic Molecules, I, II, III"; Shell Development Co.: Emeryville, CA, 1962.

(18) (a) Available from the Quantum Chemical Program Exchange, Indiana University, Bloomington, IN. We had difficulty matching the various hydrogen bending coordinates in the two sets of programs. The difficulties seem to be in the definitions of the bending interaction constants in the Cartesian program NORCRD. The definitions have been fixed by Dr. Dennis Reuter in the most recent versions of NORCRD. (b) Gwinn, W. D. *J. Chem. Phys.* **1971**, *55*, 477-81.

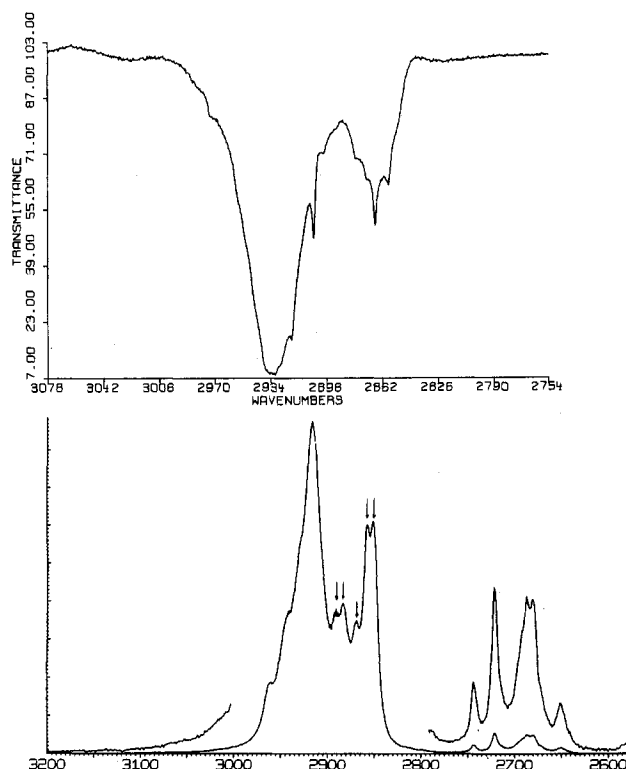


Figure 8. Bottom: Raman spectrum of cyclooctane showing methylene stretch region; Isotropic trace. The five distinct peaks in the  $\text{CH}_2$  symmetric stretching region are marked. Top: Vapor-phase infrared spectrum of cyclooctane showing methylene stretch region.

This latter program handles the vibrational problem solely in Cartesian space.

The results of calculation for boat-chair cyclooctane are shown in Table V. There is poor agreement between calculated and observed frequencies for the methylene scissors vibrations. The force field used was derived from relatively unstrained hydrocarbons and is not strictly applicable to cyclooctane. A number of the methylene bend-bend interaction constants of appreciable magnitude are defined on the basis of ideal gauche or trans relationships between HCC internal coordinates, but these ideal relationships do not exist between the methylene groups in the boat-chair.

In the high-frequency spectrum of cyclooctane, unusual splittings were observed in the C-H stretch region. The appropriate portions of the infrared and Raman spectra are shown in Figure 8. There are five resolved peaks corresponding to symmetric C-H stretches which are particularly clear in the Raman spectrum. This strongly suggests the presence of five nonequivalent methylene groups<sup>19</sup> and is, of course, consistent with the boat-chair conformation.

For the two oxocanes, the aliphatic ether force field of Snyder and Zerbi<sup>20</sup> was applied to the "boat-chair 1,3" and "boat-chair 1,3,6". The use of this optimized force field was not possible without additional assumptions, since the cyclic ethers require force constants not derived in the Snyder and Zerbi investigation of monoethers. When this situation arose, the known force constant for the coordinate most like that needed force constant was used. For example, the constant for an OCC angle bend was used for the OCO angle bend. Once again, bend-bend interaction

(19) Snyder, R. G., private communication. This conclusion is based on extensive comparison with the CH stretching region of other alkanes.

(20) Snyder, R. G.; Zerbi G. *Spectrochim. Acta, Part A* **1967**, *23*, 391-437.

TABLE V: Normal Coordinate Calculation of Cyclooctane<sup>a</sup>

no.	symmetry	$\nu_{\text{calcd}}$	$\nu_{\text{obsd}}(\text{IR gas})$	$\nu_{\text{obsd}}(\text{Raman})$	approximate motion
1	A'	2923	2933 vs	2940 vs, p	asym C-H stretch
2	A'	2920	2921 vs		asym C-H stretch
3	A'	2920			asym C-H stretch
4	A''	2920			asym C-H stretch
5	A''	2917			asym C-H stretch
6	A'	2916		2915 vvs, p	asym C-H stretch
7	A''	2914			asym C-H stretch
8	A'	2913	2908 vs		asym C-H stretch
9	A'	2869		2885 vs, p	sym C-H stretch
10	A''	2869			sym C-H stretch
11	A'	2868	2880 s	2880 vs, p	sym C-H stretch
12	A'	2868	2872 s		sym C-H stretch
13	A''	2867			sym C-H stretch
14	A'	2867	2867 s	2865 vs, p	sym C-H stretch
15	A''	2866	2859 s	2855 vs, p	sym C-H stretch
16	A'	2865	2853 s	2850 vvs, p	sym C-H stretch
17	A''	1444	1483 s	1475 s, dp	CH scissors (70), R (30)
18	A''	1416	1472 s	1462 vs, dp	CH scissors (75), R (23)
19	A'	1414	1453 s		CH scissors (78), R (22)
20	A''	1405		1442 vs, dp	CH scissors
21	A'	1404			CH scissors
22	A''	1401			CH scissors
23	A'	1398			CH scissors
24	A'	1396			CH scissors
25	A''	1395			CH wag
26	A'	1394			CH wag
27	A'	1388			CH wag
28	A''	1378			CH wag
29	A''	1370			CH wag
30	A'	1367	1364 m		CH wag
31	A''	1356	1360 m	1350 s, dp	R (13), CH wag (87)
32	A'	1349			R (13), CH wag (87)
33	A''	1300	1297 m		CH twist
34	A'	1290	1291 m	1287 vs, p	CH twist
35	A'	1260	1260 m	1255 s, p	R (20), CH twist and wag (80)
36	A''	1255	1250 m		R (15), CH twist and wag (85)
37	A''	1223	1230 m	1232 m, p	R (10), CH twist (90)
38	A'	1218		1217 m, dp	CH twist and wag
39	A''	1177	1175 vw	1170 w, dp	R (18), CH twist (82)
40	A''	1141	1137 w		R (65), CH twist (35)
41	A'	1122		1135 m, p	R (36), $\theta$ (20), CH wag (42)
42	A''	1114		1110 s, dp	CH twist
43	A''	1101	1088 vw	1082 vw, dp	R (59), mixed CH (39)
44	A'	1093			R (48), mixed CH (43)
45	A'	1020	1046 s	1045 m, p	$\theta$ (36), CH rock (55)
46	A''	972	988 w	982 vs, p	R (70), $\theta$ (10), CH rock (17)
47	A'	971	956 m	955 vs, p	R (52), CH rock (41)
48	A''	946			R (25), $\theta$ (10), CH rock (61)
49	A'	922	930 w		R (23), CH rock (70)
50	A''	844	862 m	872 m, dp	R (11), $\theta$ (13), CH rock (73)
51	A'	826	854 m	855 m, p	R (10), $\theta$ (23), CH rock (65)
52	A'	782	799 w	795 s, p	R (73), CH rock (22)
53	A''	775	768 m	760 vs, p	R (60), CH rock (34)
54	A'	730	725 w	735 m, p	R (60), CH rock (31)
55	A''	727			CH rock (88)
56	A'	669	691 w	700 vs, p	R (24), CH rock (67)
57	A'	530		667 w, p	$\theta$ (45), CH rock (45)
58	A''	467		540 vw	$\theta$ (55), CH rock (45)
59	A'	450	514 m	517 m, dp	$\theta$ (45), CH rock (55)
60	A'	390	475 <sup>b</sup> w	482 w, p	$\theta$ (50), $\tau$ (20), CH rock (30)
61	A'	352	367 <sup>b</sup> w	367 w, p	$\theta$ (60), $\tau$ (20), CH rock (20)
62	A''	352	317 <sup>b</sup> vw	326 m sh, p	$\theta$ (68), $\tau$ (15), CH rock (17)
63	A''	256	295 <sup>b</sup> vw	292 m, dp	$\theta$ (60), $\tau$ (24)
64	A'	234	255 vw	245 vw, dp	$\theta$ (64), $\tau$ (21), CH rock (13)
65	A'	138	220 vw	212 vw, p	$\theta$ (10), $\tau$ (81)
66	A''	110		125 vw, dp	$\tau$ (88)

<sup>a</sup> The motions involving the bond and torsional angles are denoted by  $\theta$  and  $\tau$ , respectively. R denotes the stretching of a C-C ring bond, and, for the cyclic ethers, S denotes a C-O stretch. The motions of the methylene group are defined with respect to the plane formed by three consecutive ring atoms, where the methylene group of interest is located at the central atom. These motions are defined as follows: scissors, the protons move out of the plane in opposite directions; twist, the protons move in the plane in opposite directions; wag, the protons move in the plane in the same direction; rock, the protons move out of the plane in the same direction. The numerical values in parentheses represent the percentage contribution of the diagonal elements of the potential energy distribution of the normal coordinate. These have been normalized to 100% and were noted if their magnitude was 10% or greater. Abbreviations: p = polarized, dp = depolarized, s = strong, m = medium, w = weak, v = very, sh = shoulder. <sup>b</sup> From condensed-phase spectrum.

TABLE VI: Normal Coordinate Calculation of 1,3-Dioxocane<sup>a</sup>

no.	symmetry	$\nu_{\text{calcd}}$	$\nu_{\text{obsd}}(\text{IR gas})$	$\nu_{\text{obsd}}(\text{Raman})$	approximate motion
1	A	2958	2966 vvs		asym C-H stretch
2	A	2958	2850 vvs		asym C-H stretch
3	A	2935	2938 vvs		asym C-H stretch
4	A	2918	2928 vvs	2930 vvs, p	asym C-H stretch
5	A	2917	2924 vvs	2910 vs, p	asym C-H stretch
6	A	2914		2900 vs, p	asym C-H stretch
7	A	2872	2892 vs		sym C-H stretch
8	A	2872	2886 vs		sym C-H stretch
9	A	2868	2874 vs	2875 s, p	sym C-H stretch
10	A	2866	2869 vs	2860 s, p	sym C-H stretch
11	A	2865			sym C-H stretch
12	A	2851		2845 s, p	sym C-H stretch
13	A	1509	1489 m		CH wag
14	A	1473	1474 m	1472 m, dp	CH scissors
15	A	1436	1455 s	1450 s, dp	CH scissors
16	A	1425	1438 m	1440 s, dp	CH scissors
17	A	1421		1432 s, dp	CH scissors
18	A	1417			CH scissors
19	A	1405	1408 m	1408 m, dp	CH scissors
20	A	1399			mixed CH
21	A	1394	1385 m	1382 vw, p	mixed CH
22	A	1377			CH wag
23	A	1360		1360 vw, p	CH wag
24	A	1318	1316 w	1314 w, dp	R (13), CH wag (89)
25	A	1296			R (14), CH twist (79)
26	A	1285	1284 s	1281 w, dp	CH wag
27	A	1273			CH wag
28	A	1260		1265 m, p	CH twist
29	A	1222	1220 m		CH twist
30	A	1217	1212 s	1217 w, p	CH twist and wag
31	A	1170	1180 s	1175 m, p	R (10), S (68), CH twist (22)
32	A	1128	1129 vvs	1118 m, p	R (29), S (53), mixed CH (14)
33	A	1099		1093 vw, dp	R (48), S (19), mixed CH (28)
34	A	1086	1089 m		R (16), S (10), $\theta$ (11), mixed CH (62)
35	A	1034	1052 vvs	1035 m, p	R (17), S (21), mixed CH (46)
36	A	1026	1018 m	1015 w, dp	$\theta$ (10), CH rock (72)
37	A	1002	976 vs	1000 vvw	R (34), S (29), CH rock (29)
38	A	979	971 s	965 s, p	R (34), S (41), CH rock (20)
39	A	899		895 wsh, dp	R (13), S (34), $\theta$ (10), CH rock (14)
40	A	884	867 m		S (12), CH rock (72)
41	A	849	859 m	860 m, p	R (43), S (31), $\theta$ (11), mixed CH (13)
42	A	809	793 m	790 m, p	R (16), $\theta$ (18), mixed CH (58)
43	A	769	754 w		R (26), S (17), CH rock (46)
44	A	738	748 w	749 m, p	R (37), CH rock (41)
45	A	642	639 m	637 vw, dp	$\theta$ (65), CH rock (20)
46	A	555	533 vw	535 vw, dp	$\theta$ (59), CH rock (32)
47	A	522	501 m	497 m, p	$\theta$ (66), CH rock (27)
48	A	438	419 vw	422 w, dp	$\theta$ (65), $\tau$ (14), CH rock (15)
49	A	387	374 <sup>b</sup> w	372 w, p	$\theta$ (68), $\tau$ (13)
50	A	355	344 <sup>b</sup> w	347 m, p	$\theta$ (62), $\tau$ (15)
51	A	276		305 vw, p	$\theta$ (72), $\tau$ (15)
52	A	257	254 <sup>b</sup> w	267 w, dp	$\theta$ (67), $\tau$ (17)
53	A	142	220 m	225 vw, p	$\theta$ (12), $\tau$ (78)
54	A	110	120 vw	135 vwsh, dp	$\tau$ (87)

<sup>a</sup> See Table V for notation. <sup>b</sup> Value taken from the condensed-phase spectrum.

force constants of  $<0.02$  mdyne/rad<sup>2</sup> were ignored in the calculations.

The results for 1,3-dioxocane are shown in Table VI and for 1,3,6-trioxocane in Table VII. Despite the various assumptions employed in the calculations, the agreement between calculated and observed vibrational frequencies is excellent. For each molecule, an abnormally high methylene wag frequency appeared. Close examination of the eigenvector revealed that it was confined to the motion of the methylene group isolated by two oxygen atoms.

The low-frequency vibrations calculated for all of the molecules cannot be expected to fit well since a harmonic potential was used in their determination. Examination of the eigenvectors reveals rather severe mixing of methylene group motions among the 10 lowest frequencies. The better fit achieved with the cyclic ethers may be due to

the substitution of oxygen atoms acting to break up methylene group interactions in the ring, thus making the ethers simpler than the parent hydrocarbon.

### Summary and Conclusions

The infrared, far-infrared, and Raman spectra of cyclooctane and two oxygenated heterocycles have been examined in detail. Special attention has been given to the low-frequency region, and the three molecules show striking similarities in their vibrational properties, leading to a reasonable hypothesis that the ring skeleton of each has the same basic structure. A number of sum and difference bands and overtones in the low-frequency spectra were noted and assigned. Close observation of the methylene stretching region in the spectra of cyclooctane suggests that the five methylene groups are nonequivalent, giving further support to a proposed boat-chair structure.

TABLE VII: Normal Coordinate Calculation of 1,3,6-Trioxocane<sup>a</sup>

no.	symmetry	$\nu_{\text{calcd}}$	$\nu_{\text{obsd}}(\text{IR gas})$	$\nu_{\text{obsd}}(\text{Raman})$	approximate motion
1	A	2962	2979 s		asym C-H stretch
2	A	2959	2960 vs		asym C-H stretch
3	A	2956		2955 vs, p	asym C-H stretch
4	A	2954	2953 vs	2945 vs, p	asym C-H stretch
5	A	2919	2932 vs	2910 vs, p	asym C-H stretch
6	A	2873	2899 s	2882 vs, p	sym C-H stretch
7	A	2872	2892 s	2877 vs, p	sym C-H stretch
8	A	2872	2885 s		sym C-H stretch
9	A	2871			sym C-H stretch
10	A	2867	2865 s	2856 vs, p	sym C-H stretch
11	A	1511	1480 w		CH wag
12	A	1471	1474 m	1467 s, dp	CH scissors
13	A	1435	1456 m	1440 vs, dp	CH scissors
14	A	1431	1436 w		CH scissors
15	A	1419		1417 m, dp	CH scissors
16	A	1415			CH scissors
17	A	1406	1409 w		CH scissors
18	A	1399			CH wag
19	A	1396	1379 m	1387 m, p	CH wag and twist
20	A	1346		1358 w, dp	CH wag
21	A	1336			CH wag and twist
22	A	1286	1297 s	1286 m, dp	mixed CH
23	A	1277	1281 s	1270 m, dp	S (14), mixed CH (83)
24	A	1264	1263 m	1254 m, dp	S (10), mixed CH
25	A	1244	1255 m	1244 m, dp	S (11), mixed CH (87)
26	A	1173	1191 s	1185 w, p	R (12), S (66), Mixed CH (20)
27	A	1134	1151 vvs	1137 s, p	R (12), S (48), CH twist (38)
28	A	1121	1126 m	1120 w, p	R (11), S (58), CH twist (33)
29	A	1098	1100 m	1092 w, p	R (12), S (26), CH rock (57)
30	A	1057	1066 s	1066 w, dp	S (10), CH twist (82)
31	A	1030	1023 w	1020 s, dp	S (35), CH twist (60)
32	A	1017	1018 m	1012 s, p	R (33), S (39), mixed CH (20)
33	A	991	995 s	987 s, p	R (33), S (37), mixed CH (25)
34	A	927	917 w	915 m, dp	S (50), $\theta$ (22), CH rock (26)
35	A	860	870 s	864 m, p	R (34), S (34), CH rock (22)
36	A	847	857 m		S (27), CH wag (66)
37	A	816	827 w	824 m, p	R (11), S (23), CH rock (52)
38	A	809	804 w	800 m, p	R (17), S (39), $\theta$ (10), CH rock (32)
39	A	664	665 w	651 w, dp	S (16), $\theta$ (64), CH rock (14)
40	A	581		542 w, dp	$\theta$ (71), CH rock (19)
41	A	558	539 w	518 w, dp	$\theta$ (73), CH rock (15)
42	A	447	440 w	460 w, p	$\theta$ (67), $\tau$ (15) CH rock (12)
43	A	401	390 m	385 m, p	$\theta$ (75), $\tau$ (14)
44	A	389	337 vw	335 vw, p	$\theta$ (72), $\tau$ (10)
45	A	280		295 w, dp	$\theta$ (75), $\tau$ (14)
46	A	273	256 w	260 w, p	$\theta$ (70), $\tau$ (18)
47	A	147	223 w	230 vw, p	$\theta$ (12), $\tau$ (82)
48	A	119	122 vw	137 vw, dp	$\tau$ (91)

<sup>a</sup> See Table V for notation.

The observed vibrational frequencies in Table V agree well with those reported by Bellis and Slowinski.<sup>3</sup>

A ring-bending potential energy expression was derived which provides information that is consistent with the energies, geometries, and low-frequency vibrations of the three rings studied. This was done at the sacrifice of some of the details of the vibrations. In particular, the model for ring-bending does not include methylene group motions, while a complete normal coordinate analysis reveals a significant contribution of methylene rocking to the low frequencies. However, the information derived from the potential is consistent with all relevant evidence from this and other investigations, with the exception of lack of evidence for the crownlike conformer of the trioxocane observed in the NMR.

The frequencies calculated from the potential function are consistent only with boat-chair structures for all three molecules. For the two cyclic ethers, pseudorotation of the ring results in geometrically distinct boat-chairs that have nearly the same ring-bending frequencies, but the oxygen

atoms show strong preferences among the nonequivalent positions on the basis of potential energy.

Complete normal coordinate analysis of cyclooctane revealed that a vibrational force field derived from unstrained *n*-alkanes was not exactly applicable to this strained hydrocarbon and that this molecule has some unusual vibrational properties that warrant further attention. However, an aliphatic ether force field applied to the two oxocanes resulted in calculated frequencies that fit beautifully with experiment.

**Acknowledgment.** We thank Professor F. A. L. Anet for advice on the syntheses and Mr. Jeff Dreyer for the preparation of one of the oxocanes. Dr. Robert G. Snyder is responsible for the beautiful Raman spectra. We thank Dr. James R. Scherer for use of his Raman spectrometer. Drs. Janet L. Offenbach and Dennis Reuter provided much assistance with the vibrational calculations. We gratefully acknowledge support from the National Science Foundation.